U.S. Department of Energy
FreedomCAR and Vehicle Technologies, EE-2G
1000 Independence Avenue, S.W.
Washington, D.C. 20585-0121

FY 2007

TEST REPORT ON Isothermal Systems Research's DOUBLE-LOOP, SPRAY-COOLED INVERTER

Prepared by:

Oak Ridge National Laboratory

Mitch Olszewski, Program Manager

Submitted to:

Energy Efficiency and Renewable Energy
FreedomCAR and Vehicle Technologies
Vehicle Systems Team

Susan A. Rogers, Technology Development Manager

January 2007

OAK RIDGE
NATIONAL LABORATORY
MANAGED BY UT-BATTELLE
FOR THE DEPARTMENT OF ENERGY

ORNL/TM-2006/622

Engineering Science and Technology Division

TEST REPORT ON Isothermal Systems Research's DOUBLE-LOOP, SPRAY-COOLED INVERTER

J. S. Hsu
C. L. Coomer
S. L. Campbell
R. H. Wiles
K. T. Lowe
M. T. McFee

Publication Date: January 2007

Prepared by the
OAK RIDGE NATIONAL LABORATORY
Oak Ridge, Tennessee 37831
managed by
UT-BATTELLE, LLC
for the
U.S. DEPARTMENT OF ENERGY
Under contract DE-AC05-00OR22725

UT-BATTELLE
ORNL-27 (4-00)

DOCUMENT AVAILABILITY

Reports produced after January 1, 1996, are generally available free via the U.S. Department of Energy (DOE) Information Bridge:

Web site: http://www.osti.gov/bridge

Reports produced before January 1, 1996, may be purchased by members of the public from the following source:

National Technical Information Service
5285 Port Royal Road
Springfield, VA 22161
Telephone: 703-605-6000 (1-800-553-6847)
TDD: 703-487-4639
Fax: 703-605-6900
E-mail: info@ntis.fedworld.gov
Web site: http://www.ntis.gov/support/ordernowabout.htm

Reports are available to DOE employees, DOE contractors, Energy Technology Data Exchange (ETDE) representatives, and International Nuclear Information System (INIS) representatives from the following source:

Office of Scientific and Technical Information
P.O. Box 62
Oak Ridge, TN 37831
Telephone: 865-576-8401
Fax: 865-576-5728
E-mail: reports@osti.gov
Web site: http://www.osti.gov/contact.html

This report was prepared as an account of work sponsored by an agency of the United States Government. Neither the United States government nor any agency thereof, nor any of their employees, makes any warranty, express or implied, or assumes any legal liability or responsibility for the accuracy, completeness, or usefulness of any information, apparatus, product, or process disclosed, or represents that its use would not infringe privately owned rights. Reference herein to any specific commercial product, process, or service by trade name, trademark, manufacturer, or otherwise, does not necessarily constitute or imply its endorsement, recommendation, or favoring by the United States Government or any agency thereof. The views and opinions of authors expressed herein do not necessarily state or reflect those of the United States Government or any agency thereof.

CONTENTS

FIGURES

TABLES

INTRODUCTION

Figure 1 shows a typical commercial implementation of an Isothermal Systems Research, Inc. (ISR) double-loop, two-phase spray cooling system. This system, utilized in a hybrid electric vehicle (HEV) automotive application could be designed to use 85ºC transmission oil to cool a heat exchanger on a second loop. The heat exchanger would function to condense the vapor back to liquid inside a sealed enclosure for continuous spray cooling of the power electronics. In Oak Ridge National Laboratory (ORNL) tests of this proposed system, 85ºC water/ethylene/glycol (WEG) was used instead of transmission oil. WEG has better thermal properties, which was the basis for selecting it over transmission oil.

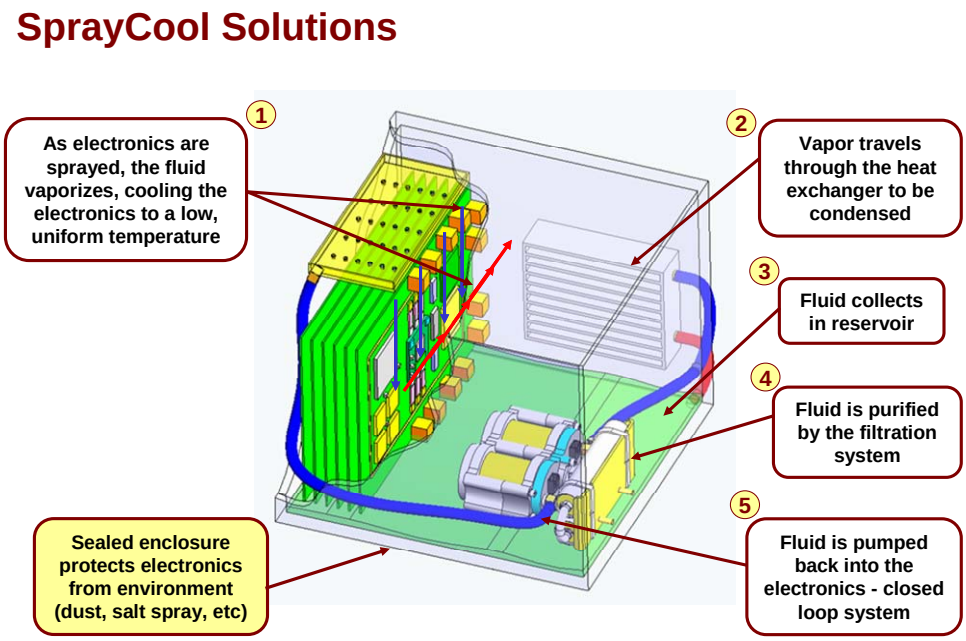

Fig. 1. Conceptual structure of an ISR spray cooling system.

The ISR system test setup that uses spray cooling to cool the IGBTs of a SemiKron inverter, and a stand alone SemiKron inverter (82kW at 70°C) is shown in Fig 2. A sealed enclosure is required to house the heat exchanger for the vapor, as shown in Fig. 3. The heat exchanger in the test was cooled by a second loop that uses 85°C WEG. Note that because the ISR spray-cooling system requires a second independent cooling loop, the final inverter may well be inherently larger than the commercial inverter utilizing a single cooling loop with a heat exchanger. The ISR test setup was constructed by modifying a standard SemiKron inverter. To accommodate the modifications it was necessary to remove the dc bus capacitors. The volume normally consumed by the capacitors was replaced by the hardware necessary for the spray nozzles.

The test results shown later in this report indicate that because the heat exchanger inside the sealed enclosure was not sufficient to maintain a liquid/vapor equilibrium at high heat loads, the pressure increased and activated the pressure safety valve at a junction temperature of 113.5ºC and an enclosure pressure of 5 psig. The test results also show that the aluminum enclosure was the major cooling source, and not the WEG heat exchanger. The aluminum enclosure did not have any external thermal insulation; therefore, the air pulled across the enclosure by the exhaust fan actually produced a cooling effect on the enclosure. This testing environment is very different from the under-hood environment, which can reach

temperatures of 140°C. In short, the substitution of WEG for transmission oil and the active cooling provided by the aluminum enclosure caused the cooling conditions for the test to be better than conditions that would exist in a real automotive environment.

Before the load test was initiated, the ISR test setup was placed inside an environmental chamber to obtain the collector-emitter voltage vs temperature curves for each insulated gate bipolar transistor (IGBT) under a very low predetermined test current (9 mA for a total of 18 IGBT chips).

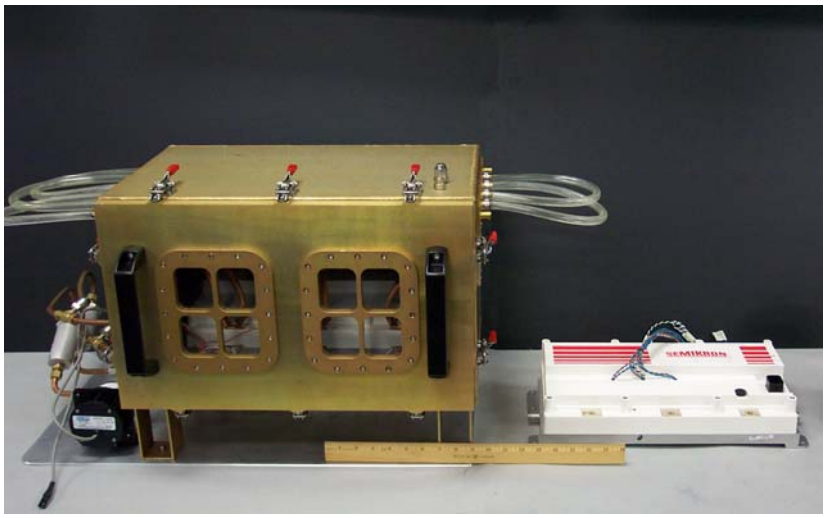

Fig. 2. ISR spray cooling system test setup with Semikron commercial inverter.

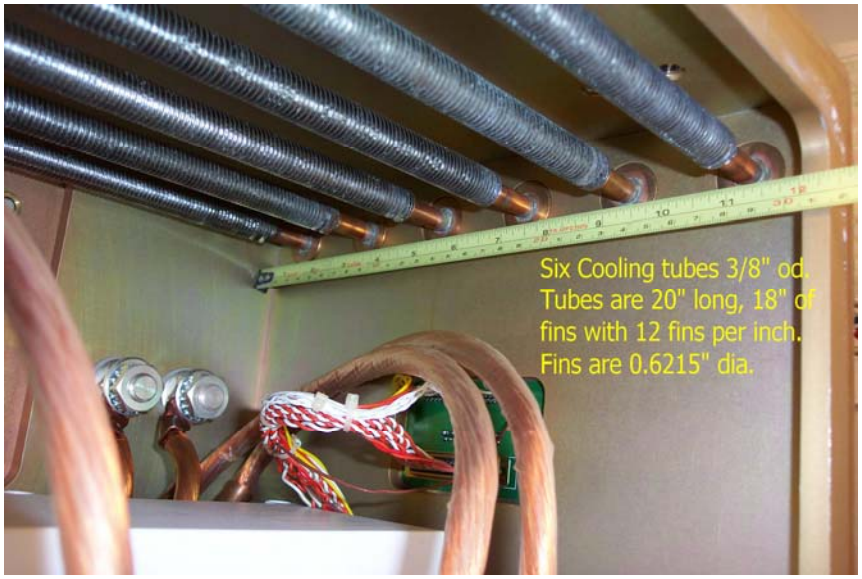

Fig. 3. Heat exchanger consisting of six cooling tubes.

The pressure gauge of the sealed enclosure was calibrated as shown in Fig. 4. To prepare the enclosure for testing, the air had to be evacuated from the chamber because of the flammable nature of the spray coolant. A7 psia vacuum was drawn down on the sealed container and then purged with nitrogen to 14.7 psia. After three rounds of this procedure, a vacuum was drawn to 7 psia, and 3800 ml of cooling

fluid was released into the aluminum enclosure. Three additional rounds of vacuum/pressure purges were performed. As a final step, a vacuum was pulled to 7 psia and a 9-psia nitrogen purge was conducted. The inverter system was then ready for testing.

Fig. 4. Calibration of pressure sensor with gauge.

Figure 5 depicts the ORNL test arrangement during the load test of the ISR test setup. For safety considerations, the ISR test setup was placed inside a ventilation chamber with an additional half-inch-thick piece of Lexan between the inverter and the safety-glass sash door. This arrangement was required to meet physical, chemical, and mechanical safety requirements.

Fig. 5. Inverter placed inside the ventilation chamber.

A dc chopper circuit, shown in Fig. 6, was used for simultaneously loading all the IGBTs in the three legs of the inverter. The temperature readings took place when the chopper provided zero load current to the

inverter. The chopper frequency was around 10 cycles per second with 90 ms on and 9.4 ms off. The IGBT temperature reading took place when the chopper current was off. The IGBTs were heated during the 90 ms on time. The very short 9.4 ms off time, during which the readings were made, did not cause significant cooling of the IGBTs.

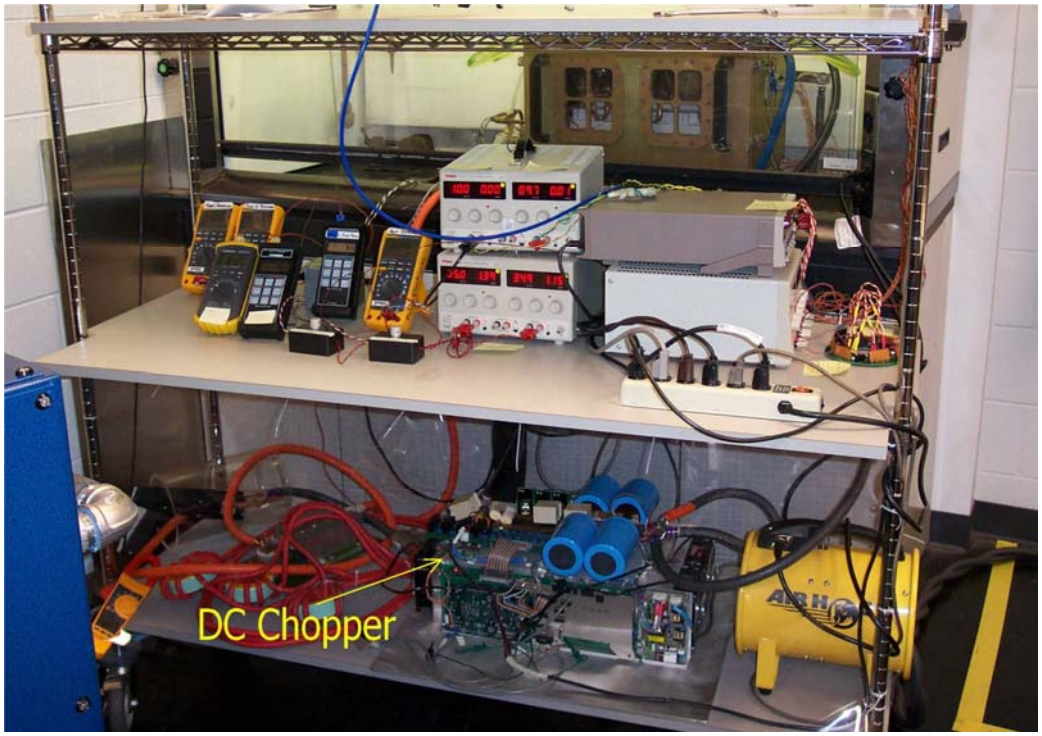

Fig. 6. The dc chopper used during testing.

Figure 7 shows the arrangement of the upper spray nozzles. Eighteen nozzles were used to spray the tops of 18 IGBTs. A separate set of 18 nozzles (not shown) were provided to spray the bottoms of the IGBTs. The test was conducted with both sides actively cooled.

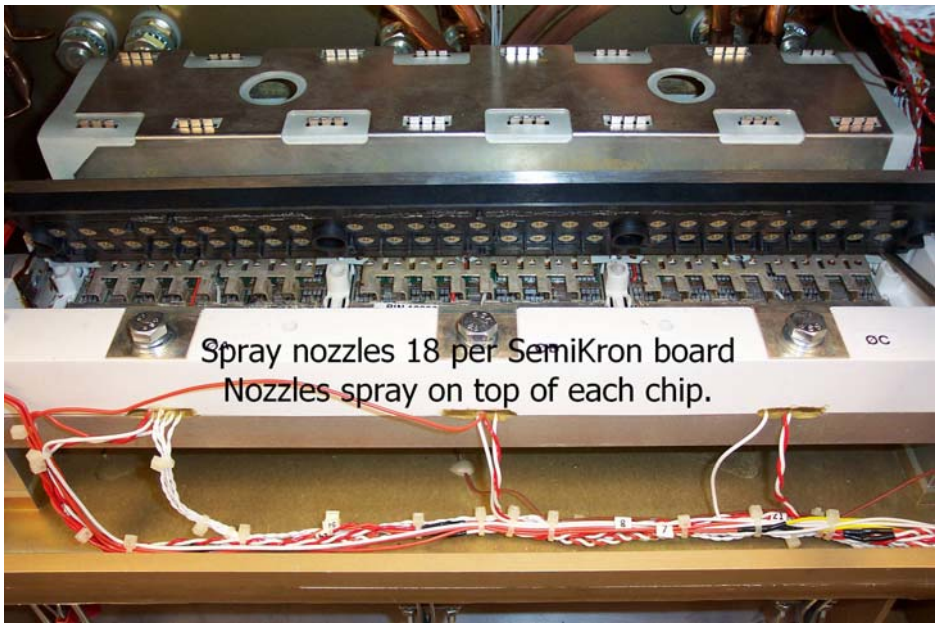

Fig. 7. Arrangement of upper spray nozzles.

Figure 8 shows the two micropumps rated at 36V, 3A, which provided a maximum power rating of 100W and were used for pumping fluid through the upper and lower nozzles. Their corresponding filters and pressure sensors are also shown in Figure 8.

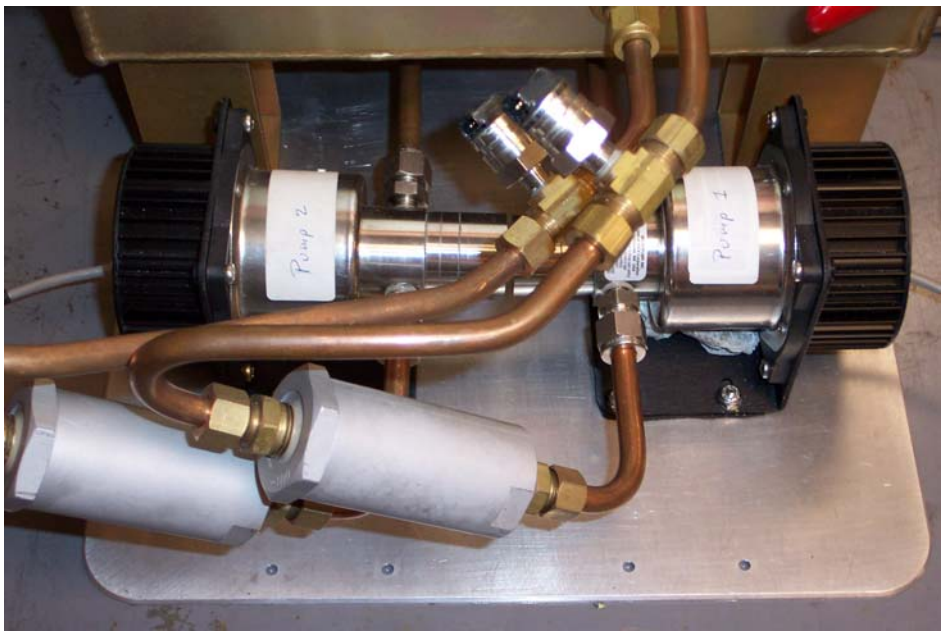

Fig. 8. Two micropumps utilized for the upper and lower nozzles.

Figure 9 shows the chopper current and the junction temperature traces during the test.

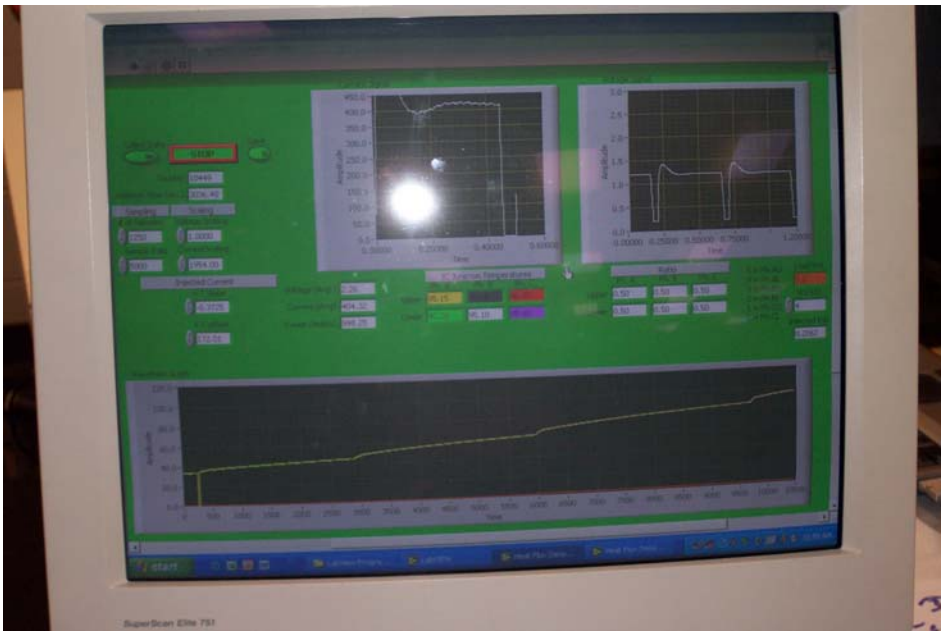

Fig. 9. Chopper current and junction temperature traces.

The plot of temperature vs time and the projected stabilized maximum temperatures for 30A and 400A loads, respectively, are shown in Fig. 10. The projected maximum stabilized temperature, $T_{\infty,}$ is estimated by Eq. (1):

$$T = T_0 + (T_\infty - T_0)(1 - e^{-t/C}) \ , \tag{1}$$

where *t* is the time measured from the initial time corresponding to the initial temperature, T_0, and the time constant *C* is a constant. Any error from the calculated quantity in Eq. (1) is caused by the fact that the junction is cooled through multiple layers of different materials. The junction thermal model is represented by a relatively complicated structure function. Using Eq. (1) the projected maximum stabilized temperatures are 94.6°C and 113.5°C for the 300A and 400A loads, respectively. The test was halted during the 400A load test because the safety valve was actuated by the pressure built up inside the enclosure.

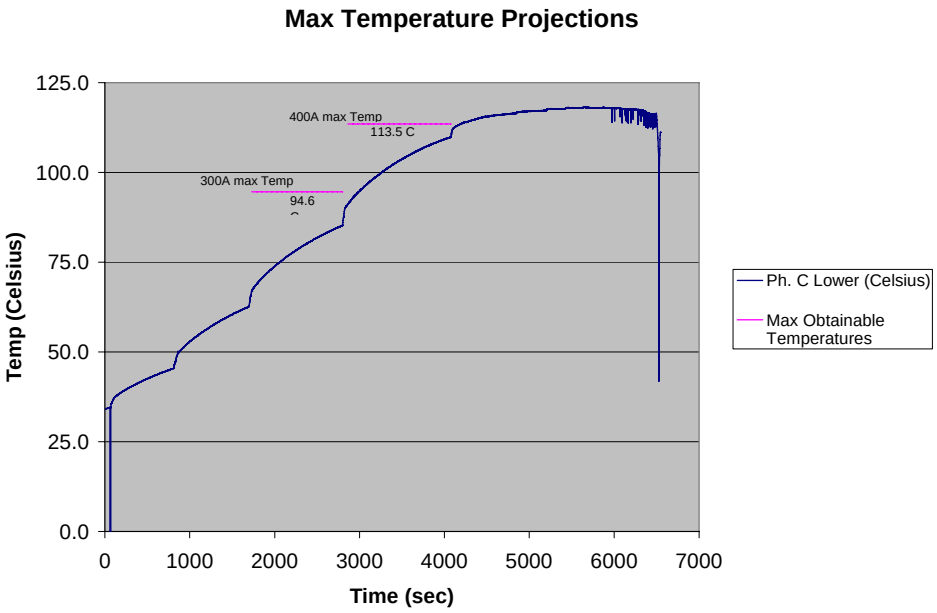

Fig. 10. Junction temperature and projected stabilized maximum temperature.

Table 1 shows that during load situations not exceeding 400A, the WEG inlet temperature was higher than the WEG outlet temperature. This meant the 85°C WEG heat exchanger was not cooling the inverter and became a thermal load on the inverter. Only when the load was higher than 400A with a higher coolant temperature, and the release valve actuated, did the WEG heat exchanger start to cool the two-phase coolant.

Table 1. WEG temperatures, flow rates, and pressures for second-loop cooling

Time [sec]	WEG [gal/min]	WEG outlet [C]	WEG inlet [C]	WEG ΔP [psi]
1735	2.69	84.4	85.3	17
2350	2.69	84.4	85.3	17
2750	2.68	84.5	85.4	17
2830	2.66	84.7	85.6	17
3510	2.65	84.7	85.4	17
3950	2.71	84.7	85.3	17
4100	2.63	84.7	85.4	17
5460	2.69	85	85.3	17
6410	2.7	85.5	84.5	17

Table 2 shows the cooling power of the WEG heat exchanger. The negative heat exchanger power confirms the previous assertion that the 85°C WEG heat exchanger became a thermal load to the inverter. The inverter relied strongly on the cooling provided by the huge aluminum enclosure located inside the ventilation chamber. Note that in a hybrid vehicle, the inverter is situated under the hood, where the dependency on the enclosure cooling may be problematic. The calculation example of the dissipation power of the WEG heat exchanger for the first data line of Table 2 is shown in the Appendix.

Table 2. Data for calculation of cooling dissipation power of the WEG heat exchanger

Time (sec)	Inlet (F)	Outlet (F)	Delta (ºF)	Flow Liter/sec	Spec heat $(\frac{BTU}{lb\cdot^{\circ}F})$	Spec gravity (kg/L)	$\frac{W}{BTU/\sec}$	lb/kg	Exchanger (W)
1735	185.5	183.9	–1.6	0.1697	0.8575	1.044	1054	2.2	–563.6
2350	185.5	183.9	–1.6	0.1697	0.8575	1.044	1054	2.2	–563.6
2750	185.7	184.1	–1.6	0.1691	0.8575	1.044	1054	2.2	–561.6
2830	186.1	184.5	–1.6	0.1678	0.8575	1.044	1054	2.2	–557.3
3510	185.7	184.5	–1.3	0.1672	0.8575	1.044	1054	2.2	–451.2
3950	185.5	184.5	–1.1	0.1710	0.8575	1.044	1054	2.2	–390.5
4100	185.7	184.5	–1.3	0.1659	0.8575	1.044	1054	2.2	–447.7
5460	185.5	185	–0.5	0.1697	0.8575	1.044	1054	2.2	–176.1
6410	184.1	185.9	+1.8	0.1703	0.8575	1.044	1054	2.2	+636.3

Table 3 shows the capabilities for IGBT cooling at various temperature differences between the IGBT junction and the low pressure refrigerant. The cooling reached approximately 34 W/cm² before the release valve was actuated. The projected maximum steady junction temperature at 403 A, 995 W is 113.5°C. There is no doubt that the current loading could go higher than 403A while maintaining a junction temperature of 125°C if the pressure buildup inside the enclosure could be prevented by improving the second-loop cooling.

Table 3. Capabilities for IGBT cooling

Time (sec)	dc (A)	dc (V)	Power (W)	IGBT W/cm²	IGBT ΔT°C	Coolant fluid temperature (°C)	Pumps (W)	Upper nozzle psia	Lower nozzle psia	Container (psia)
1735	302.8	2.09	686.96	23.6	11.58	55.4	99.75	45	44	13
2350	302.2	2.08	682.36	23.4	12.78	66.7	98.7	45	44	14.4
2750	302.1	2.08	681.14	23.4	17.73	72.0	94.15	45	45	15.2
2830	405.6	2.27	1002.02	34.4	17.25	72.5	92.4	45	45	15.4
3510	403.6	2.26	998.06	34.2	17.21	86.2	88.9	45	44	17.2
3950	403.8	2.26	994.90	34.1	16.59	91.8	87.15	44	44	18.6
4100	453.6	2.35	1165.10	40.0	18.77	93.0	92.05	45	44	18.7
5460	510.8	2.45	1368.14	46.9	15.93	101.6	138.95	30.6	42	18.7
6410	603.2	2.61	1721.38	59.0	13.54	102.4	134.05	29.3	40	18.3

Table 4 shows the relationship between WEG inlet temperatures, low pressure coolant fluid temperatures, and total IGBT losses. To begin the test, 3800 ml of coolant fluid was placed in the unit. Enclosure pressure data indicate that the vapor started to escape at t= 3950 seconds. After the test, 3460 ml of coolant was recovered.

Table 4. WEG inlet temperatures, low-pressure coolant fluid temperature, and total IGBT loss

Time (sec)	WEG inlet (°C)	Coolant fluid temperature (°C)	Total IGBT loss (W)	Cooling power of exchanger (W)
1735	85.3	55.4	686.96	–563.6
2350	85.3	66.7	682.36	–5763.6
2750	85.4	72.0	681.14	–561.6
2830	85.6	72.5	1002.02	–557.3
3510	85.4	86.2	998.06	–451.2
3950	85.3	91.8	994.90	–390.5
4100	85.4	93.0	1165.10	–447.7
5460	85.3	101.6	1368.14	–176.1
6410	84.5	102.4	1721.38	+636.3

CONCLUSIONS

The ISR double-loop, two-phase spray cooling system was designed to use 85ºC transmission oil to cool a heat exchanger via a second cooling loop. The heat exchanger condenses the working fluid vapor back to liquid inside a sealed enclosure to allow for continuous spray cooling of electronics. In the ORNL tests, 85ºC WEG, which has better thermal properties than transmission oil, was substituted for the transmission oil.

Because the ISR spray-cooling system requires a second cooling loop, the final inverter might be inherently larger than inverters that do not require a second-loop cooling system. The ISR test setup did not include a dc bus capacitor. Because the IGBT conduction test indicated that the ISR test setup could not be properly loaded thermally, no switching tests were conducted. Therefore it was not necessary to attach external capacitors outside the test setup.

During load situations not exceeding 400A, the WEG inlet temperature was higher than the WEG outlet temperature. This meant that the 85°C WEG heat exchanger was not cooling the inverter and became a thermal load to the inverter. Only when the load was higher than 400A with a higher coolant temperature and the release valve actuated did the WEG heat exchanger start to cool the 2-phase coolant. The inverter relied strongly on the cooling of the huge aluminum enclosure located inside the ventilation chamber. In a hybrid vehicle, the inverter is situated under the hood, where the dependency on cooling provided by the enclosure may become a problem.

The IGBT power dissipation with both sides being spray cooled was around 34 W/cm² at 403A, with 995W total IGBT loss at 113.5°C projected junction temperature before the release valve was actuated. The current loading could rise higher than 403 A before reaching the 125°C junction temperature limit if the pressure buildup inside the enclosure could be prevented by improving the secondary cooling loop. This 34 w/cm2 was an average across all dies.

There is no doubt that the cooling capability of the ISR spray-cooling test setup can be improved by (1) lowering the WEG inlet temperature from 85°C to say 70°C, this would condense the vapor better and lower the container pressure, (2) modification of the vapor condenser inside the container to cool both the vapor and the liquid of the 2-phase coolant, in the present setup only the vapor is cooled by the condenser inside the container, and (3) lower the liquid temperature through (1) and (2) to avoid the vaporization that causes cavitations in the pump for ensuring the pump's life expectance.

APPENDIX

Example for Calculation of Cooling Power of WEG Heat Exchanger

The specific gravity and the specific heat capacity for the 50% water ethylene glycol coolant solution at various temperatures are given as follows.

Specific gravity of ethylene-glycol–based water solutions SG (% by volume) (kg/L)	
Temperature (°F)	50% by volume
–40	
0	1.1
40	1.088
80	1.077
120	1.064
160	1.05
200	1.038

Specific heat capacity of ethylene-glycol–based water solutions (Btu/lb·°F)	
Temperature (°F)	50% by volume
–40	
0	0.78
40	0.795
80	0.815
120	0.832
160	0.85
200	0.865

The cooling power of the WEG heat exchanger can be calculated through the following equation:

(WEG outlet temp – WEG outlet temp) × flow × specific heat × specific gravity × W/BTU/sec × lb/kg = exchanger (W).

For an example, substituting the values of the first data line of Table 2 into the equation gives

$$(183.9°\text{F}–185.5°\text{F}) \times 0.1697\frac{Liter}{\sec} \times 0.8575\frac{BTU}{lb\cdot{}^{\circ}F} \times 1.044\frac{kg}{Liter} \times 1054\frac{W}{BTU/\sec} \times 2.2\frac{lb}{kg} = -563.6\ \text{W}.$$

DISTRIBUTION

Internal

1. D. J. Adams
2. S. L. Campbell
3. C. L. Coomer
4. E. C. Fox
5. K. P. Gambrell
6. J. S. Hsu
7. K. T. Lowe
8. L. D. Marlino
9. M. T. McFee
10. M. Olszewski
11. R. H. Wiles
12. Laboratory Records

External

13. R. Al-Attar, DCX, raa9@dcx.com.
14. T. Q. Duong, U.S. Department of Energy, EE-2G/Forrestal Building, 1000 Independence Avenue, S.W., Washington, D.C. 20585.
15. R. R. Fessler, BIZTEK Consulting, Inc., 820 Roslyn Place, Evanston, Illinois 60201-1724.
16. K. Fiegenschuh, Ford Motor Company, Scientific Research Laboratory, 2101 Village Road, MD-2247, Dearborn, Michigan 48121.
17. V. Garg, Ford Motor Company, 15050 Commerce Drive, North, Dearborn, Michigan 48120-1261.
18. G. Hagey, Sentech, Inc., 501 Randolph St., Williamsburg, Virginia 23185.
19. E. Jih, Ford Motor Company, Scientific Research Laboratory, 2101 Village Road, MD-1170, Rm. 2331, Dearborn, Michigan 48121.
20. K. J. Kelly, National Renewable Energy Laboratory, 1617 Cole Boulevard, Golden, Colorado 80401
21. A. Lee, Daimler Chrysler, CIMS 484-08-06, 800 Chrysler Drive, Auburn Hills, Michigan 48326-2757.
22. F. Liang, Ford Motor Company, Scientific Research Laboratory, 2101 Village Road, MD1170, Rm. 2331/SRL, Dearborn, Michigan 48121.
23. M. W. Lloyd, Energetics, Inc., 7164 Columbia Gateway Drive, Columbia, Maryland 21046.
24. M. Mehall, Ford Motor Company, Scientific Research Laboratory, 2101 Village Road, MD-2247, Rm. 3317, Dearborn, Michigan 48124-2053.
25. J. A. Montemarano–Naval Surface Warfare Center, Carderock Division; Code 642, NSWCD, 9500 MacArthur Boulevard; West Bethesda, Maryland 20817
26. N. Olds, United States Council for Automotive Research (USCAR), nolds@uscar.org
27. J. Rogers, Chemical and Environmental Sciences Laboratory, GM R&D Center, 30500 Mound Road, Warren, Michigan 48090-9055.
28. S. A. Rogers, U.S. Department of Energy, EE-2G/Forrestal Building, 1000 Independence Avenue, S.W., Washington, D.C. 20585.
29. G. S. Smith, General Motors Advanced Technology Center, 3050 Lomita Boulevard, Torrance, California 90505.
30. E. J. Wall, U.S. Department of Energy, EE-2G/Forrestal Building, 1000 Independence Avenue, S.W., Washington, D.C. 20585.
31. B. Welchko, General Motors Advanced Technology Center, 3050 Lomita Boulevard, Torrance, California 90505.
32. P. G. Yoshida, U.S. Department of Energy, EE-2G/Forrestal Building, 1000 Independence Avenue, S.W., Washington, D.C. 20585.